



ARL-TR-8869 • DEC 2019



Alloying Behavior and Crystallinity of (111)-Oriented Lead Tin Telluride Grown on (100)-Oriented Gallium Arsenide

by Vijay Parameshwaran and Patrick Taylor

Approved for public release; distribution is unlimited.

NOTICES

Disclaimers

The findings in this report are not to be construed as an official Department of the Army position unless so designated by other authorized documents.

Citation of manufacturer's or trade names does not constitute an official endorsement or approval of the use thereof.

Destroy this report when it is no longer needed. Do not return it to the originator.



Alloying Behavior and Crystallinity of (111)-Oriented Lead Tin Telluride Grown on (100)-Oriented Gallium Arsenide

by Vijay Parameshwaran and Patrick Taylor
Sensors and Electron Devices Directorate, CCDC Army Research Laboratory

REPORT DOCUMENTATION PAGE

Form Approved
OMB No. 0704-0188

Public reporting burden for this collection of information is estimated to average 1 hour per response, including the time for reviewing instructions, searching existing data sources, gathering and maintaining the data needed, and completing and reviewing the collection information. Send comments regarding this burden estimate or any other aspect of this collection of information, including suggestions for reducing the burden, to Department of Defense, Washington Headquarters Services, Directorate for Information Operations and Reports (0704-0188), 1215 Jefferson Davis Highway, Suite 1204, Arlington, VA 22202-4302. Respondents should be aware that notwithstanding any other provision of law, no person shall be subject to any penalty for failing to comply with a collection of information if it does not display a currently valid OMB control number.

PLEASE DO NOT RETURN YOUR FORM TO THE ABOVE ADDRESS.

1. REPORT DATE (DD-MM-YYYY) December 2019		2. REPORT TYPE Technical Report		3. DATES COVERED (From - To) October 2018-September 2019	
4. TITLE AND SUBTITLE Alloying Behavior and Crystallinity of (111)-Oriented Lead Tin Telluride Grown on (100)-Oriented Gallium Arsenide				5a. CONTRACT NUMBER	
				5b. GRANT NUMBER	
				5c. PROGRAM ELEMENT NUMBER	
6. AUTHOR(S) Vijay Parameshwaran and Patrick Taylor				5d. PROJECT NUMBER	
				5e. TASK NUMBER	
				5f. WORK UNIT NUMBER	
7. PERFORMING ORGANIZATION NAME(S) AND ADDRESS(ES) US Army Combat Capabilities Development Command Army Research Laboratory ATTN: FCDD-RLS-EM Adelphi, MD 20783				8. PERFORMING ORGANIZATION REPORT NUMBER ARL-TR-8869	
9. SPONSORING/MONITORING AGENCY NAME(S) AND ADDRESS(ES)				10. SPONSOR/MONITOR'S ACRONYM(S)	
				11. SPONSOR/MONITOR'S REPORT NUMBER(S)	
12. DISTRIBUTION/AVAILABILITY STATEMENT Approved for public release; distribution is unlimited.					
13. SUPPLEMENTARY NOTES primary author's email: <vijay.s.parameshwaran.civ@mail.mil>.					
14. ABSTRACT Ternary lead tin telluride (Pb _x Sn _{1-x} Te) alloy films are grown on (100)-oriented gallium arsenide (GaAs) substrates with molecular beam epitaxy in order to achieve a heteroepitaxial system that enables technological innovations for IR photonics, thermoelectrics, and topological insulators. X-ray diffraction is used to study the crystallinity of this ternary alloy and its epitaxial nature in relation to the GaAs substrate. Symmetric 2θ-ω scans across the alloy range and a reciprocal space map (RSM) of a ternary Pb _x Sn _{1-x} Te compound confirm an epitaxial growth, with a (111)-oriented film on a (100)-oriented substrate. Broadening in reciprocal space within the RSM makes it difficult to determine an in-plane lattice constant or strain, but evidence indicates that the film is relaxed. This work enables innovations in future growth for Group IV-VI materials on III-V substrates to develop technologies in the aforementioned application space.					
15. SUBJECT TERMS molecular beam epitaxy, lead tin telluride, gallium arsenide, x-ray diffraction					
16. SECURITY CLASSIFICATION OF:			17. LIMITATION OF ABSTRACT UU	18. NUMBER OF PAGES 19	19a. NAME OF RESPONSIBLE PERSON Vijay S Parameshwaran
a. REPORT Unclassified	b. ABSTRACT Unclassified	c. THIS PAGE Unclassified			19b. TELEPHONE NUMBER (Include area code) 301-394-0927

Contents

List of Figures	iv
List of Tables	iv
1. Introduction	1
2. Experimental Methods	2
2.1 MBE Growth	2
2.2 XRD Measurement and Analysis	2
3. Results and Discussion	4
3.1 Qualitative Analysis	4
3.2 Quantitative Analysis	6
4. Summary and Conclusions	9
5. References	10
List of Symbols, Abbreviations, and Acronyms	11
Distribution List	13

List of Figures

Fig. 1	Symmetric 2θ - ω scan of the three samples under study	4
Fig. 2	RSM scan of the ternary PbSnTe sample under study	5
Fig. 3	Symmetric 2θ - ω scan of the three samples under study, zoomed in to view the (222) PbSnTe diffraction peaks	7

List of Tables

Table 1	Calculation of the lattice constants from the (222) PbSnTe peaks in the symmetric scan.....	7
Table 2	Variations in the extracted lattice constant from the (002) RSM scan for ternary PbSnTe.....	8

1. Introduction

The ternary lead tin telluride ($\text{Pb}_x\text{Sn}_{1-x}\text{Te}$) alloy, as a part of the Group IV-VI materials system, is a material that has use in a variety of applications such as long-wavelength (8–15 μm) IR photonic devices,¹ topological insulators,² and thermoelectrics.³ The ability to control the synthesis of this material through molecular beam epitaxy (MBE) opens up several possibilities for innovations in these application areas by growing on heterogeneous substrates and designing structures with quantum wells and superlattices. While most historical work on crystal growth of this materials system has been on similar substrates, which have a rocksalt cubic crystal structure such as lead telluride (PbTe), this work investigates the growth of $\text{Pb}_x\text{Sn}_{1-x}\text{Te}$ on gallium arsenide (GaAs), which is a zincblende cubic crystal that is a part of the III-V materials system.

GaAs substrates are more readily available as compared to Group IV-VI substrates due to their proliferation within the semiconductor photonics and electronics industry, and the heterogeneous integration of epitaxial $\text{Pb}_x\text{Sn}_{1-x}\text{Te}$ on GaAs can enable the demonstration of the novel physics in this materials system within a III-V processing line that can scale up the technology readiness level (TRL) similar to the line of research that aims to integrate IR detector material onto silicon as a prevalent and widespread semiconductor substrate. GaAs has a zincblende cubic structure with a lattice constant of 5.653 Å. In contrast, the lattice constants of SnTe and PbTe, which have a rocksalt cubic structure, are nominally 6.30 and 6.46 Å, respectively.

This work aims to achieve two goals: 1) MBE growth of $\text{Pb}_x\text{Sn}_{1-x}\text{Te}$ on GaAs, and 2) X-ray diffraction (XRD) analysis of the heterogeneous materials system with the aim of gaining a full understanding of the nature of the epitaxy, alloying, crystallinity, and strain within the grown material. With this knowledge, further growth experiments can be carried out in order to better control the physical properties of $\text{Pb}_x\text{Sn}_{1-x}\text{Te}$ for enabling future technologies in photonics, topological insulators, and thermoelectrics.

Although XRD can be used as a technique to identify the phase, orientation, and alloying based on the “fingerprint” of a 2θ angle indexed to a powder diffraction pattern, in this work, more careful analysis is required. The $\text{Pb}_x\text{Sn}_{1-x}\text{Te}$ system exhibits a relatively high coefficient of thermal expansion that can distort the lattice.^{4,5}

Moreover, thin $\text{Pb}_x\text{Sn}_{1-x}\text{Te}$ layers are grown, so there exists a possibility of strain coherency through pseudomorphic growth on a GaAs substrate.

2. Experimental Methods

2.1 MBE Growth

Growth of the $\text{Pb}_x\text{Sn}_{1-x}\text{Te}$ materials is performed on (100) GaAs substrates with a 4° miscut. The substrates are loaded into the MBE system and their surfaces were thermally cleaned at high temperatures under a fluence of tellurium dimers, and then cooled to the growth temperature of 275°C . Prepared in this way, the surface before epitaxial growth possesses a tellurium-passivated, or Ga_2Te_3 -rich chemistry.

The pure compounds, PbTe and SnTe, are grown using flux values from the individual constituents (tin metal, lead metal, and dimeric tellurium) and the composition of the $\text{Pb}_x\text{Sn}_{1-x}\text{Te}$ alloys is controlled by individually adjusting the relative fluence values of Pb and Sn. The flux ratio of the group VI element (tellurium) to the group IV elements (Pb, Sn) is typically maintained at a VI/IV ratio of 40. This is a unique MBE process in that alloys in this system are usually grown by congruent sublimation of the parent compounds (PbTe and SnTe), whereas in this specific MBE chamber, the constituent elements each have their own crucible.⁶

During growth, reflection-high-energy-electron-diffraction (RHEED) is used to show consistently (1X1) unreconstructed surfaces for all materials.

Within the scope of this study, three samples are analyzed to view the crystal behavior of the alloy: binary PbTe, binary SnTe, and ternary $\text{Pb}_x\text{Sn}_{1-x}\text{Te}$.

2.2 XRD Measurement and Analysis

XRD measurements are done on a PANalytical X'Pert Pro system, with a $1/2^\circ$ incident beam slit, a mirror system to focus the incident X-ray beam, a 4-bounce germanium (Ge) [220] monochromator to filter the incident X-ray radiation such that only the $\text{Cu } K\alpha_1$ wavelength (1.5402 \AA) is incident on the material. A PIXCel detector is used to enable electronic and software adjustment of the effective "receiving slit" during alignment and measurements, and to enable an integrated collection measurement in reciprocal space for relatively fast and high-quality scans.

Two types of measurements are performed on the material: a symmetric 2θ - ω scan

and a reciprocal space map (RSM). In a symmetric scan, both 2θ and ω are varied over a range such that θ is equal to ω and the scattering vector \mathbf{q} is perpendicular to the sample surface. For the epitaxially grown films in this work, the 2θ - ω scan range is set to a value such that the $(00l)$ peaks of the substrate and the corresponding film peaks are viewable. The 2θ value corresponding to the peak is extracted, and the out-of-plane lattice constant a_{\perp} is calculated through Bragg's Law

$$\lambda = 2d \sin \theta. \quad (1)$$

and the equation

$$\frac{1}{d_{\perp}^2} = \frac{h^2 + k^2 + l^2}{a_{\perp}^2}, \quad (2)$$

which is specific to crystals with cubic phases. h , k , and l are the indices corresponding to the specific crystal plane being analyzed, and d_{\perp} is the out-of-plane crystal plane spacing calculated from the θ diffraction angle through Bragg's Law:

$$\lambda = 2d_{\perp} \sin \theta. \quad (3)$$

The RSM is a two-dimensional XRD scan that aligns \mathbf{q} to a crystal plane that is off-axis to the surface normal. It validates and further characterizes the epitaxial nature of a film grown on a single-crystal substrate. The RSM has the 2θ - ω direction as one axis, and the ω direction as the other axis. These data can be re-visualized as the out-of-plane scattering vector q_{oop} on one axis, and the in-plane scattering vector q_{ip} on the other axis.

These data are interpreted through the relations

$$q_{oop} = \frac{\lambda}{2d_{\perp}}, q_{ip} = \frac{\lambda}{2d_{\parallel}}, \quad (4)$$

with d_{\parallel} as the in-plane crystal lattice spacing.

3. Results and Discussion

3.1 Qualitative Analysis

Figure 1 shows the symmetric XRD scans of the three samples under study, showing the relevant diffraction peaks. Under a wide-angle scan with the 2θ values varying from 20° to 80° (not shown), the only viewable peaks are the $\{001\}$ family of planes for the zincblende cubic GaAs substrate that were allowed by its structure factor, and the $\{111\}$ family of planes for the rocksalt cubic $\text{Pb}_x\text{Sn}_{1-x}\text{Te}$ system that were allowed by its structure factor. Therefore, from these results, it can be inferred that the growth is epitaxial in nature, with (111)-oriented $\text{Pb}_x\text{Sn}_{1-x}\text{Te}$ on (100)-oriented GaAs.

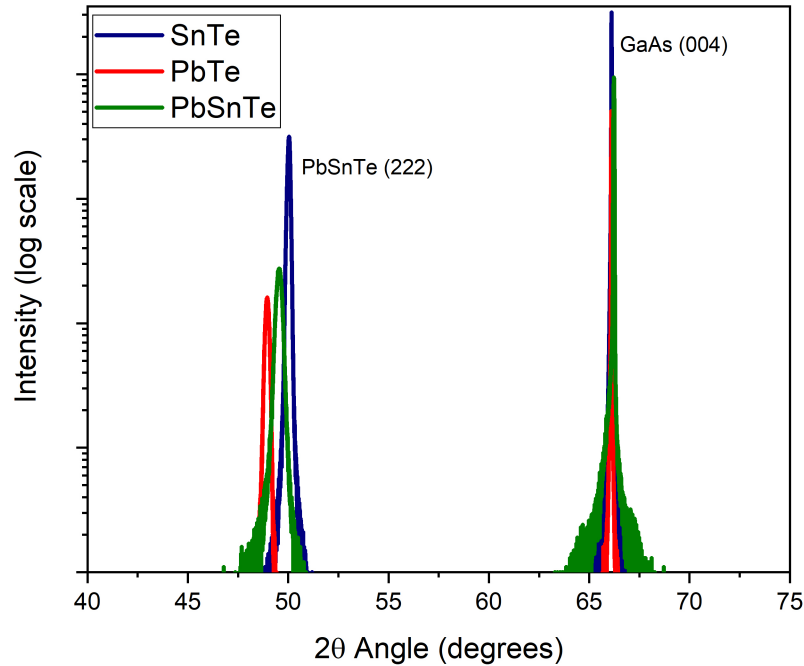


Fig. 1 Symmetric 2θ - ω scan of the three samples under study

The symmetric scan, however, is not a complete analysis to determine that the $\text{Pb}_x\text{Sn}_{1-x}\text{Te}$ alloy is epitaxial on GaAs, especially since this is a relatively unconventional example of a (111)-oriented cubic film on a (100)-oriented cubic substrate. The reason this description is incomplete is because the scattering vector q

only measures the out-of-plane crystallinity, with no indicator of the in-plane crystallinity. Hence, an RSM is required to elucidate the exact nature of the film.

Figure 2 shows the RSM of the (002) off-axis reflection of the ternary PbSnTe sample in this study. Due to the alignment specifications within the PANALYTICAL X'Pert Pro system, Q_y is not shown as the out-of-plane scattering vector perpendicular to the surface normal, but instead is the scattering vector parallel to the [002] crystallographic direction. Similarly, Q_x is not shown as the in-plane scattering vector parallel to the surface normal, but instead is shown as the scattering vector perpendicular to the [002] crystallographic direction.

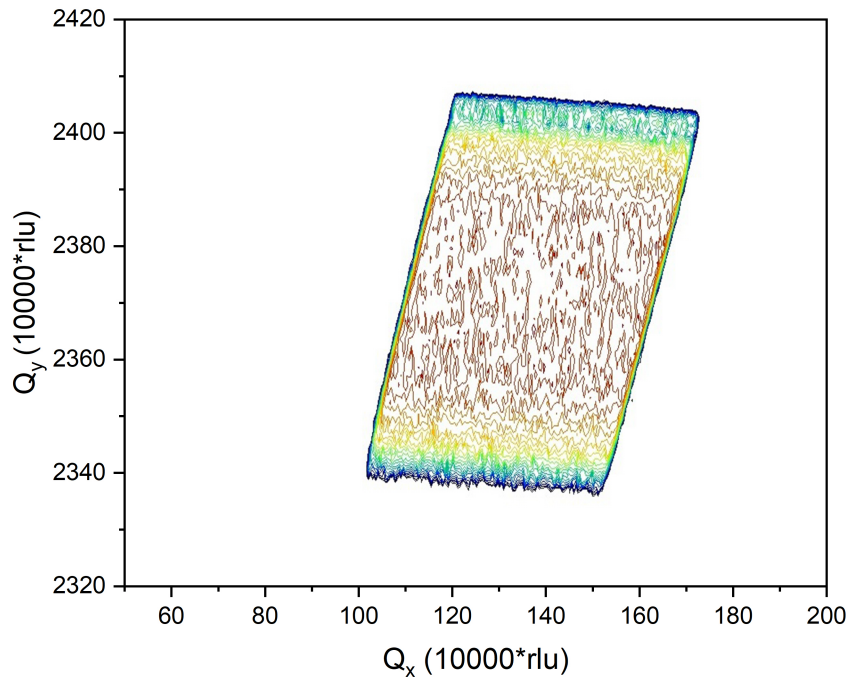


Fig. 2 RSM scan of the ternary PbSnTe sample under study

From the RSM plot, three conclusions can be obtained. First, the PbSnTe (002) reflection is an isolated peak in reciprocal space, indicating that the scattering vector shows single-crystallinity in both its in-plane and out-of-plane components, thus confirming that the MBE growths achieved epitaxial single-crystal (111)-oriented PbSnTe on (100)-oriented GaAs. Second, while the PbSnTe (002) reflection is proof

of single-crystal material, the nonzero values of Q_x across the diffraction peak indicate some nonzero amount of tilt or distortion from the cubic lattice. Third, the spatial divergence in both the Q_x and Q_y directions show that there is some amount of mosaicity within the film. In diffraction theory, an ideal crystal would be a single point (or delta function) in reciprocal space, with broadening related primarily to finite crystal size and texturing/mosaicity. Furthermore, the amount of broadening in this crystal makes it impossible to extract a single point in reciprocal space to determine the lattice constant from the (002) reflection.

Another feature of this scan is that atypical of most RSM diffraction peaks, the intensity profile is not a Gaussian or Lorentzian type function, but instead a constant value in a parallelogram-type shape, similar to a mesa. One could imagine that this profile is limited by the optics and measurement parameters of the diffractometer, but other materials have been analyzed in the same configuration that did not show this profile. It should be noted that the off-axis alignment was complicated by the 4° miscut on the GaAs substrate and low absolute intensity of the (002) reflection, both of which could contribute to the non-ideal measurement. Nevertheless, it remains that the XRD measurements confirmed epitaxial growth of (111)-oriented PbSnTe on (100)-oriented GaAs.

3.2 Quantitative Analysis

Figure 3 shows a zoomed-in plot of the (222) reflections of the three film samples (PbTe, SnTe, and PbSnTe) from Fig. 1. As an indicator of the broadening of the RSM in Fig. 2, all three peaks show a broadening within the symmetric direction. The PbTe film has a full width at half maximum (FWHM) value of 880.02 arcsec, the SnTe film has a FWHM value of 549.756 arcsec, and the PbSnTe film has a FWHM value of 1189.8 arcsec. Although broadening in this direction is related primarily to finite crystal size rather than mosaicity, it could help explain similar broadening within the RSM.

To quantify the crystal parameters within the grown materials, the lattice constants of all three compounds were extracted by using Bragg's Law and the relation

$$\frac{1}{d^2} = \frac{h^2 + k^2 + l^2}{a^2}, \quad (5)$$

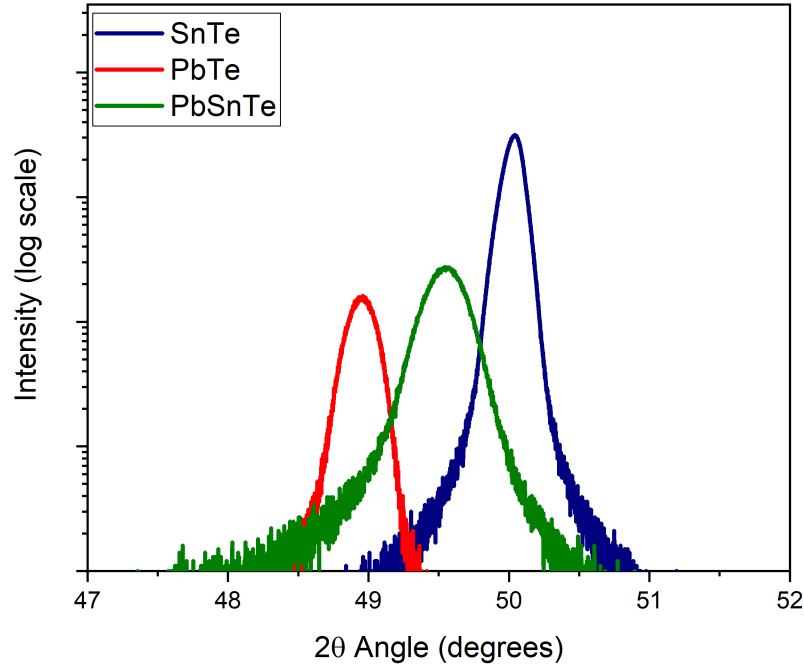


Fig. 3 Symmetric 2θ - ω scan of the three samples under study, zoomed in to view the (222) PbSnTe diffraction peaks

which holds for all cubic lattices. Since the (222) reflections are used for analysis, the values of h , k , and l are set to be 2. Since, for all scans, there is a slight deviation from the nominal 2θ value for the GaAs (004) reflection corresponding to its lattice constant of 5.653 \AA , a correction was made for the 2θ values for the film diffraction peaks by incorporating a $\Delta 2\theta$ offset. The results are shown in Table 1.

Table 1 Calculation of the lattice constants from the (222) PbSnTe peaks in the symmetric scan

Material	2θ ($^\circ$)	θ ($^\circ$)	d (\AA)	a (\AA)
PbTe	48.847	24.4235	1.863	6.4536
SnTe	49.986	24.993	1.823	6.3150
PbSnTe	49.377	24.6885	1.8442	6.3885

The alloy fraction for the PbSnTe sample is determined by applying Vegard's Law, which has been historically shown to accurately describe this materials system⁷ :

$$a_{\text{Pb}_x\text{Sn}_{1-x}\text{Te}} = xa_{\text{PbTe}} + (1 - x)a_{\text{SnTe}}. \quad (6)$$

From this analysis and the lattice constants from Table 1, the ternary alloy has 53% Pb and 47% Sn. This assumes that there is no residual strain on the material, either from pseudomorphic growth or thermal expansion. Pseudomorphic growth is unlikely due to the difference in lattice constants and crystal orientation between the film and substrate, and thermal effects are minimal as the diffraction was performed at room temperature.

To quantitatively show how the RSM broadening in Fig. 2 makes it difficult to analyze the lattice and crystal in the (002) reflection, five points within the peak (center and four corners) were taken and analyzed by extracting the d -spacing from the scattering vector Q_y

$$2d = \frac{\lambda}{Q_y} \quad (7)$$

and using the cubic lattice relation described earlier. The results are shown in Table 2.

Table 2 Variances in the extracted lattice constant from the (002) RSM scan for ternary PbSnTe

Point	Q_x (10000*rlu)	Q_y (10000*rlu)	a (Å)
Center	134.567	2372.478	6.492
Bottom Left	100.349	2339.945	6.582
Bottom Right	150.341	2335.995	6.593
Top Left	120.098	2407.289	6.398
Top Right	171.065	2404.132	6.406

From these results, it is clear that a single lattice constant cannot be obtained, although they are all roughly in the vicinity of the lattice constants within the $\text{Pb}_x\text{Sn}_{1-x}\text{Te}$ alloy system. Interestingly enough, three of these obtained lattice constants (from the center, bottom left, and bottom right) are beyond the range of the $\text{Pb}_x\text{Sn}_{1-x}\text{Te}$ alloy. Therefore, any extended analysis is not possible with the RSM.

4. Summary and Conclusions

In summary, this work gives a comprehensive XRD study of MBE-grown (111)-oriented $\text{Pb}_x\text{Sn}_{1-x}\text{Te}$ on (100)-oriented GaAs, both binary and ternary alloyed, in order to determine the crystal structure and epitaxial relationship between the materials. This heterogeneous materials integration can enable innovations within the application space of thermoelectrics, IR photonics, and topological insulators.

Although these studies provide important insights to the heteroepitaxy of the ternary $\text{Pb}_x\text{Sn}_{1-x}\text{Te}$ alloy on (100)-oriented GaAs, the 4° miscut combined with the orientation of a (111) cubic film on a (100) cubic substrate limits the XRD analysis. Additionally, the wide range observed for both Q_x and Q_y in the RSM indicates that the film might either be too thin or that the film might not exhibit enough crystallinity; this assessment is in agreement with the wide broadening of the symmetric scan film peaks. A thicker film with higher crystallinity would, in principle, yield a more highly resolvable peak in reciprocal space from which a single scattering vector corresponding to the lattice constant can be obtained.

To further investigate the crystal structure of these films, three options exist: using Raman spectroscopy to view the bonding state of the material, using synchrotron-based X-ray scattering to view a two-dimensional map of all diffraction peaks in reciprocal space, and using transmission electron microscopy selected area diffraction to also obtain a pattern in reciprocal space. XRD, in conjunction with a heating/cooling stage, can also prove to be a valuable tool to view the thermal expansion behavior of the $\text{Pb}_x\text{Sn}_{1-x}\text{Te}$ alloy system on GaAs as a future extension of analyzing this materials system.

5. References

1. Walpole JN, Calawa AR, Harman TC. Double-heterostructure PbSnTe lasers grown by molecular-beam epitaxy with CW operation up to 114 K. *Applied Physics Letters*. 1976;28(9):552–554.
2. Liang T, Kushwaha S, Kim J, Gibson Q, Lin J, Kioussis N, Cava RJ, Ong NP. A pressure-induced topological phase with large Berry curvature in $\text{Pb}_{1-x}\text{Sn}_x\text{Te}$. *Science Advances*. 2017;3(5):1–7.
3. Orihashi M, Noda Y, Chen LD, Goto T, Hirai T. Effect of tin content on thermoelectric properties of p-type lead tin telluride. *Journal of Physics and Chemistry of Solids*. 2000;61:919–923.
4. Novikova S, Abrikosov N. Investigation of the thermal expansion of lead chalcogenides. *Soviet Physics of the Solid State*. 1964;5(7):1397–1398.
5. Houston B, Strakna B, Belson H. Elastic constants, thermal expansion, and Debye temperature of lead telluride. *Journal of Applied Physics*. 1968;39(8):3913–3916.
6. Harman T, Taylor PJ, Walsh M, LaForge B. Quantum dot superlattice thermoelectric materials and devices. *Science*. 2002;297(5590):2229–2232.
7. Bis RF, Dixon JR. Applicability of Vegard’s Law to the $\text{Pb}_{1-x}\text{Sn}_x\text{Te}$ alloy system. *Journal of Applied Physics*. 1969;40(4):1918–1921.

List of Symbols, Abbreviations, and Acronyms

TERMS:

III-V – binary compound of a Group III element (e.g., gallium, indium) and a Group V element (e.g., arsenic, phosphorus)

IV-VI – binary compound of a Group IV element (e.g., lead, tin) and a Group VI element (e.g., selenium, tellurium)

Cu $K\alpha_1$ – notation for a specific wavelength of X-ray emitted from a copper block, corresponding to an atomic orbital transition

FWHM – full width at half maximum

GaAs – gallium arsenide

Ge – germanium

IR – infrared

MBE – molecular beam epitaxy

Pb – lead

PbSnTe – lead tin telluride

PbTe – lead telluride

RHEED – reflection-high-energy-electron diffraction

RSM – reciprocal space map

Sn – tin

SnTe – tin telluride

TRL – technology readiness level

XRD – X-ray diffraction

MATHEMATICAL SYMBOLS:

Å – angstrom

arcsec – arcseconds (degrees multiplied by 3600)

Δ – offset difference

λ – wavelength (specifically, of the X-ray)

ω – diffracted angle of an X-ray on a flat surface

θ – incident angle of an X-ray on a flat surface

a – lattice constant

a_{\perp} – out-of-plane lattice constant

d – crystal plane spacing

d_{\perp} – out-of-plane crystal plane spacing

h,k,l – indices corresponding to a crystallographical direction in the Cartesian coordinate system

q – scattering vector in reciprocal space

q_{ip} – in-plane scattering vector

q_{oop} – out-of-plane scattering vector

Q_x – scattering vector in the x-direction

Q_y – scattering vector in the y-direction

x – alloy fraction

- 1 DEFENSE TECHNICAL
(PDF) INFORMATION CTR
DTIC OCA

- 1 DIR CCDC ARL
(PDF) FCDD RLD CL
TECH LIB

- 2 DIR CCDC ARL
(PDF) V PARAMESHWARAN
P TAYLOR